Carter, J. D., Cheng, G. & Guo, T. Growth of self-aligned crystalline cobalt silicide nanostructures from Co nanoparticles. J. Phys. Chem. B. 108, 6901-6904

ARTICLE *in* CHEMINFORM · APRIL 2004

Impact Factor: 0.74 · DOI: 10.1021/jp0499326

THE JOURNAL OF PHYSICAL CHEMISTRY B

 VOLUME 108, NUMBER 22, JUNE 3, 2004

LETTERS

Growth of Self-Aligned Crystalline Cobalt Silicide Nanostructures from Co Nanoparticles

Joshua D. Carter, Guangjun Cheng, and Ting Guo*

Department of Chemistry, One Shields Avenue, University of California, Davis, California 95616

Received: January 6, 2004; In Final Form: March 26, 2004

We have developed a new method with which we can for the first time produce self-aligned cobalt silicide ($CoSi_2$) nanostructures from Co nanoparticles. These nanostructures are formed by reacting Co nanoparticles with Si substrates at 900 °C. Their dimensions are normally 3 to 10 nm wide and up to a few micrometers long. The orientations of these nanostructures are controlled by the crystalline substrate, as they are orthogonally and hexagonally aligned on Si(100) and Si(111), respectively. Because these self-aligned nanostructures (SAN) are thermally stable up to 1000 °C in air and chemically inert to prolonged treatment with strong acids, and because their sizes are uniform and much smaller than those made from lithography, they can be ideal materials for making components such as electric contacts, interconnects, and gates for future nanoelectronics.

One dimensional crystalline materials such as carbon nanotubes and nanowires made of ZnO, GaN, InP, and Si have been the focus of many studies in the past decade.[1−3] Challenges to the applications of these materials arise not only from making them but also from manipulating them to form devices. It is thus advantageous if one can directly produce desired nanostructures on suitable substrates for device fabrication. Such methods are usually called a bottom-up approach, and the starting materials are often monolayers or sub-monolayers of atoms.[4−7] Lithography, on the other hand, is a top-down method. It relies on the making and breaking of large, uniform materials such as thin films. Thus, if crystalline films are available, lithography can also be used to make microstructures.[8−10] For example, using this top-down method, submicrometer cobalt silicide structures have been made.[10−15] These structures can be used as contacts, gates, and interconnects in microelectronics because cobalt silicides are an excellent conductor and are thermally and chemically stable. However, the dimensions of the structures so fabricated using the top-down approach are much larger than those of the nanotubes and nanowires mentioned above.

We report here a new method to directly synthesize as small as sub-5 nm and uniform $CoSi_2$ self-aligned nanostructures (SAN) with the bottom-up approach. Instead of using layers of atoms, our method uses nanoparticles (NP) of different sizes. The products are silicide crystalline nanostructures aligned on Si wafers.

Co nanoparticles were made by following the reported procedure.[16] In brief, 0.54 g of $Co_2(CO)_8$ was dissolved in 3-mL of oxygen-free, anhydrous dichlorobenzene in a drybox. The solution was then injected into a mixture of oleic acid, trioctylphosphine oxide, and trioctylamine at a temperature slightly above the boiling point of dichlorobenzene under Ar. After several minutes, portions of the solution were withdrawn from the reaction flask and placed in Ar-filled vials. Depending on the ratios of the surfactants, different sized Co nanoparticles were made, and their sizes were verified by transmission electron microscopy (TEM).

Figure 1a shows a TEM image of nanoparticles under a condition that favors the growth of 12-nm nanoparticles. Smaller nanoparticles are also present in the sample. The large ones

* Corresponding author. Phone: (530)-754-5283. E-mail: tguo@ucdavis.edu.

10.1021/jp0499326 CCC: $27.50
Published on Web 04/30/2004

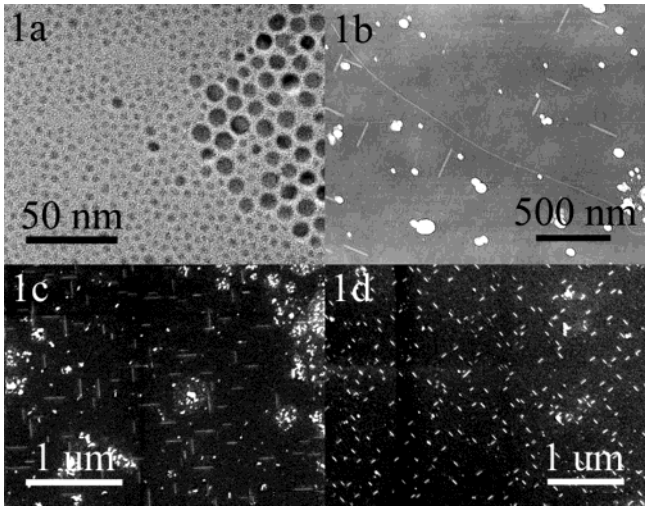

Figure 1. Images of NP and SAN. (a) TEM image of the NP. Two sizes (12 ± 1.2 nm and 4.4 ± 0.5 nm) are observed. (b) AFM image of NP and SAN. A SWNT is also visible. Long and short SAN are present, although long SAN are more visible. The height of the SAN is 3 nm and that of the SWNT is 1.4 nm. (c) Typical result of the SAN synthesized. Both long and short SAN are visible. (d) SEM image of SAN under optimized conditions. Only one length of SAN is observed, 78 ± 11 nm. The density of the SAN is 20 μm^{-2}.

have an average diameter of 12 ± 1.2 nm, and the small ones have an average diameter of 4.4 ± 0.5 nm. More uniformly sized 3- or 5-nm nanoparticles can be made using this method under a different condition, and they have been used to make SAN as well.

Deposition of the nanoparticles on Si substrates was carried out in air. The Si substrates were cleaned in a Piranha solution (1:4 H_2O_2 (30% in water) and H_2SO_4 (concd)) for 10 min before deposition. A solution containing Co nanoparticles was diluted (10:1 to 100:1) in anhydrous, oxygen-free dichlorobenzene in the drybox, and cleaned Si substrates were immersed in the diluted solution for several minutes under sonication. Deionized water and dichlorobenzene were used to wash the deposited substrates. Undoped (100) and (111) and highly B- and P-doped (100) substrates (Virginia Semiconductor) were used.

The nanoparticle-coated Si substrates were placed in a high-temperature tube furnace (Lindburg/Mini-Mite) for SAN synthesis. Ar (99.997%, 600 sccm), H_2 (99.95%, 400 sccm), and CH_4 (99.999%, 400 sccm) gases were used, and a total pressure of 1.05 bar was maintained during the reaction. Growth time varied from less than 1 s to ~2 h at different reaction temperatures. After the growth, the furnace was cooled to room temperature, and samples were examined with TEM, scanning electron microscopy (SEM), and atomic force microscopy (AFM).

Figure 1b shows the AFM (tapping mode) image of a typical SAN sample. To prepare this sample, a diluted (100:1 in dichlorobenzene) 5-nm Co nanoparticle solution and undoped Si (100) were used. The growth temperature was 1000 °C. SAN of two general lengths are observed. The long SAN have an average length of 167 ± 32 nm, and the short ones have an average length of 37 ± 2.0 nm. A single-walled carbon nanotube (SWNT) is also visible, running across the whole image. The heights of the SAN and the single-walled carbon nanotubes, both visible in this picture, are 3 ± 0.5 and 1.4 nm, respectively.

Figure 1c shows an SEM image of a SAN sample produced under a similar condition. Again, SAN of two lengths are visible: the medium (200 ± 20 nm) and short (85 ± 12 nm) SAN. On the basis of the SEM measurements, which have a resolution of 2 nm, the width of the short SAN is less than 6 nm. None of the SAN have separated metal catalysts attached to their ends.

A few long SAN, up to a few micrometers in length and with nanoparticles attached, were also observed. Their width, however, varied from 5 to 10 nm to as big as 20 nm. These long SAN have a similar morphology as those observed by Liu and colleagues.[17]

Under optimized conditions, more uniform SAN were made. Figure 1d shows SAN made using another 5-nm nanoparticle sample at 900 °C. These SAN in this sample have an average length of 78 ± 11 nm. The density is 20 SAN/μm^2, the highest produced to date.

Both N- and P-doped Si (100) substrates were used, and the yields of SAN on these substrates were similar. SAN were found aligned on either (111) or (100) surfaces. On the (111) surface, they are hexagonally aligned, forming either a 60° or 120° angle between the SAN. We have treated those SAN in air at temperatures up to 1100 °C. They were stable up to 1000 °C in air for over 2 h.

Micro-Raman spectroscopy using 785-nm light was performed on the sample shown in Figure 1b, and a peak at 1600 cm^{-1} (G band) was often observed. However, this signal could come from the single-walled carbon nanotubes present in the sample, as shown in Figure 1b. No signal from SiC was observed, as no peaks around 800 cm^{-1} were present.

High-resolution TEM was used to examine the lateral dimension and the structure of the SAN. Standard dimpling and ion milling techniques were employed. A high-resolution TEM image is shown in Figure 2a along the Si[110] zone axis. Both the substrate and the SAN have clearly resolved lattice fringes, and both fringes have ~3.8 Å spacing. Figure 2b shows two parallel SAN, indicating that they are perfectly aligned. These SAN correspond to the short SAN shown in Figure 1. Figure 2c gives the diffraction pattern of the Si sample shown in Figure 2a. The pattern agrees with that of the α-Si fcc structure ($a =$ 5.428 Å) along the 110 zone axis. No other obvious diffraction spots or rings are visible. This suggests that the crystalline structure of the SAN is very close to that of Si and is the clearest indication that the SAN has $CoSi_2$ crystals because the two have almost the same crystalline structure. The 3.8 Å spacings observed in Figure 2a further suggest that they are both (110) planes. Thus, the $CoSi_2$ SAN are grown along the [110] direction with their edges exposed on Si (100) as shown in Figures 1 and 2. In fact, such preferred growth can be explained by the fact that both (100) and (110) of $CoSi_2$ are a good match to Si (100).[10]

We have also carried out angular dependence measurements on these SAN with TEM (parts d and e of Figure 2). TEM results from two angles are shown. The image shown in Figure 2d was taken with the sample tilted −30°, rotating around the vertical axis of the image. Notice that some of the SAN are narrow, whereas others are broad. The thickness of the narrow SAN is 3 nm. Figure 2e shows an image taken at a +45° tilt angle. Those same narrow SAN become broader, and the originally broad ones become narrower. This indicates that the SAN have a sheet form with only their edges exposed above the surface. The average cross section of those SAN is 20 nm (H) × 3 nm (W). Since the surface normal to the substrate in these two measurements is not parallel to the e-beam, the overall length looks shorter than the real values. Furthermore, the sheet plane of the SAN is parallel to Si(110) and not perpendicular to the Si(100), as shown in Figure 2a.

The crystalline cobalt silicide $CoSi_2$ ($Fm3m$) has a lattice constant of 5.365 Å, very close to that of Si of 5.428 Å ($Fm3m$),

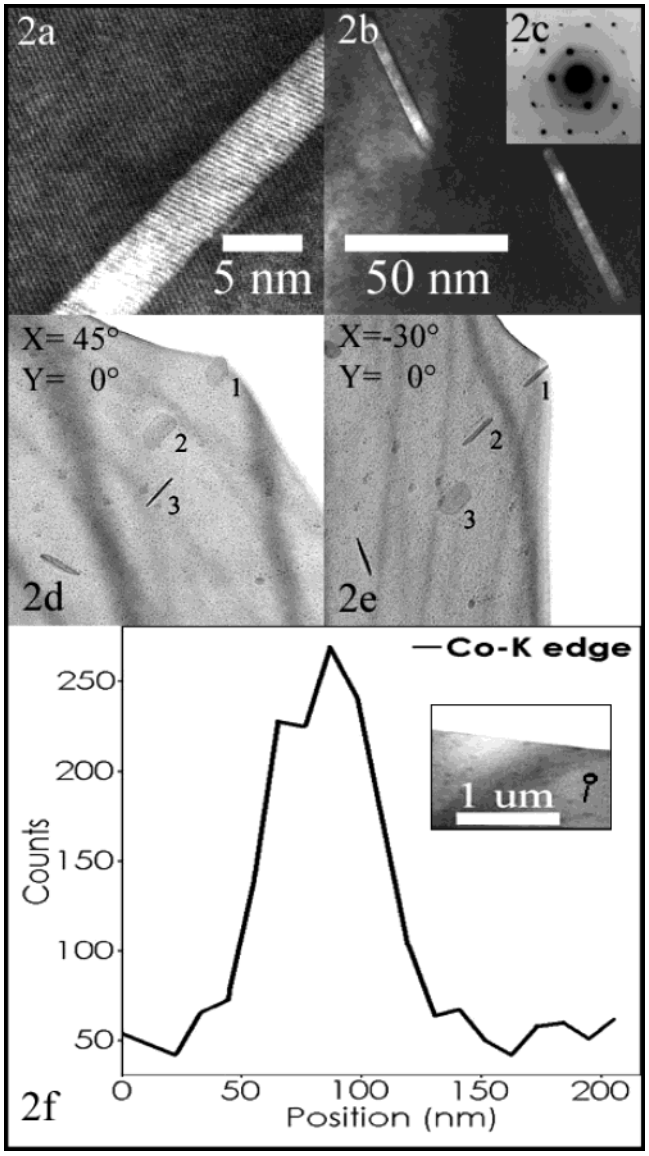

Figure 2. TEM images of SAN. (a) The atomic fringes of both the Si substrate and that of a SAN, along the Si [110] zone axis. (b) Two parallel SAN, 3.5 nm wide and 70 nm long. (c) The electron diffraction pattern of the material shown in 3a. The 2-fold symmetry from the Si [110] zone axis is shown. (d) An angular dependence TEM measurement of SAN taken at +33°. (e) The TEM image of the same sample taken by rotating 75° along the vertical line. (f) EDX of a single SAN from an ion milled SAN sample. The Co K signal is used for obtaining the lineout. The fwhm of the lineout is ~50 nm. The inset shows the location of the EDX scanning line.

thus giving a −1.17% lattice mismatch at room temperature.[18] Crystalline $CoSi_2$ is normally made at ~900 °C, the same temperature as the SAN is made in our case. At 900 °C the lattice mismatch decreases to 1.05%, favoring even more the epitaxial growth of $CoSi_2$. In addition, crystalline $CoSi_2$ is also stable in air at up to 1000 °C. However, other forms of cobalt silicides do exist. Nonetheless, Co_2Si (*Pnma*) and CoSi (*P*2*i*3) have different structures, and they are low-temperature phases or precursors that are more stable at <500 °C.[10] Furthermore, these two phases are less stable than $CoSi_2$ when interacting with bulk Si.[19] Although $CoSi_2$ can also be polycrystalline at high temperatures, the SAN observed here are single crystalline. Based on these results, we conclude that the material of the SAN is made of $CoSi_2$. Together with the electron diffraction data, we conclude that the SAN is made of crystalline $CoSi_2$.

Energy-dispersive X-ray spectroscopy measurements on these SAN also indicate the presence of Co, as shown in Figure 2f, which shows that the SAN contains Co over its entire dimension. The composition of Co in Si is ~2% because the Si signal includes that from the substrate as well as that from the $CoSi_2$ portion. The data shown in Figure 2f clearly indicate that the Co profile shares the same dimension as that of the SAN. This clearly shows that SAN are Co-containing species, not the surface intrusions.[20]

Although the morphology of these SAN resembles that of carbon nanotubes when they are characterized only with SEM and AFM, our results have shown that they are crystalline cobalt silicides. The high yield of these silicides indicates that its growth is much more energetically favorable than the formation of carbon nanotubes, which may explain why the yield of nanotubes is low. We suspect that the surfactants on the Co nanoparticles, the size of Co nanoparticles, and the type of nanoparticles all play a role in determining the most favorable growth routes, whether it is for carbon nanotubes or SAN. For example, we have observed SAN of different lengths and widths. These results can be explained by considering that the SAN are made from two sizes of nanoparticles: the larger ones (12 nm) make the long SAN and the small ones (3−5 nm) make the short SAN. It is thus worth pointing out that based on our studies it is very likely that most of the nanoparticle samples we have made contain mixed sizes, even though each size may have a small standard deviation as indicated by the TEM results.

We have presented here a different method for synthesizing this new type of nanostructure on silicon and other substrates. This approach is afforded by the limited supply from Co nanoparticles and a possibly new energetics that governs the reactions and interactions of nanoparticles with the substrate. In the conventional top-down method of making $CoSi_2$ structures, large amounts of Co (e.g., 20 nm thick layers) are deposited on Si wafers to produce single-crystalline $CoSi_2$.[10] A two-step reaction is then employed. First, CoSi is made at the Co−Si interface at 500 °C. To guarantee aligned growth of $CoSi_2$, extra Co above the interface is chemically removed before the reaction at a higher temperature is carried out, or a thin layer of other elements such as Ti is deposited. Afterward, the temperature is raised to ~700 to 900 °C to convert CoSi to $CoSi_2$ through Si migration. In our case, due to the limited supply of Co from Co nanoparticles, the mixing of Co with Si may be completed relatively quickly, and crystalline $CoSi_2$ is formed when the mixture is treated at 900 °C. It is worth noting that although the lattices of $CoSi_2$ and Si are closely matched, the boundary between the two phases is well-defined around the SAN as shown in Figure 2a. This can be explained by (1) the anisotropy of the substrate, (2) the size of the reactants (nanoparticles), (3) the slow reaction rate of Co and Si, (4) carbon surfactants that block the Co diffusion in Si, and (5) slow surface diffusion of Co on Si.[21,22] We have observed aligned migration of Co nanoparticles at lower temperatures (500 °C) as others have reported.[23]

In summary, we have synthesized the smallest Co silicide nanostructures, and they may be important to many applications. Since these SAN can be directly fabricated on Si wafers, and they are thermally and chemically stable while being potentially conductive,[24] it is possible to make different devices such as chemical sensors, interconnects between other components, and anchors for building other nanostructures. More importantly, since it is much easier to control the locations of nanoparticles than atoms, it is more practical to use this method to control the morphology of the SAN. Our method can also be easily

extended to building other types of SAN of different elements such as semiconducting crystalline iron silicides.[10,25] Future work includes a better control over the dimensions of the SAN, the types of the SAN, and the integration of different SAN to form more complex devices.

Acknowledgment. The authors are grateful to Dr. V. Puntes and Professor A. P. Alivisatos, Director of the Molecular Foundry, which is supported by the Department of Energy. We thank the staff at the National Center for Electron Microscopy, especially Dr. C. Song, for their experimental assistance. The authors thank Professor B. Casey for providing the AFM and R. Porter, F. Shan, and D. Masiel for performing the Raman measurements. This work is partially supported by an NSF CAREER award (CHE0135132) and the Camille and Henry Dreyfus Foundation. Acknowledgment is made to the donors of the Petroleum Research Fund, administrated by the American Chemical Society, for partial support of this research.

References and Notes

(1) Iijima, S.; Ichihashi, T. *Nature* **1993**, *364*, 737−737.
(2) Hu, J. T.; Odom, T. W.; Lieber, C. M. *Acc. Chem. Res.* **1999**, *32*, 435−445.
(3) Kong, Y. C.; Yu, D. P.; Zhang, B.; Fang, W.; Feng, S. Q. *Appl. Phys. Lett.* **2001**, *78*, 407−409.
(4) Viernow, J.; Lin, J. L.; Petrovykh, D. Y.; Leibsle, F. M.; Men, F. K.; Himpsel, F. J. *Appl. Phys. Lett.* **1998**, *72*, 948−950.
(5) Chen, Y.; Ohlberg, D. A. A.; Medeiros-Ribeiro, G.; Chang, Y. A.; Williams, R. S. *Appl. Phys. Lett.* **2000**, *76*, 4004−4006.
(6) Liu, B. Z.; Nogami, J. *J. Appl. Phys.* **2003**, *93*, 593−599.
(7) Ragan, R.; Chen, Y.; Ohlberg, D. A. A.; Medeiros-Ribeiro, G.; Williams, R. S. *J. Cryst. Growth* **2003**, *251*, 657−661.
(8) Rhee, H. S.; Ahn, B. T. *Appl. Phys. Lett.* **1999**, *74*, 3176−3178.
(9) Kluth, P.; Zhao, Q. T.; Winnerl, S.; Lenk, S.; Mantl, S. *Microelectron. Eng.* **2002**, *64*, 163−171.
(10) Reader, A. H.; Vanommen, A. H.; Weijs, P. J. W.; Wolters, R. A. M.; Oostra, D. J. *Rep. Prog. Phys.* **1993**, *56*, 1397−1467.
(11) Maex, K. *Mater. Sci. Eng., R* **1993**, *11*, 53−153.
(12) Moshfegh, A. Z.; Hashemifar, S. J.; Akhavan, O. *Solid State Commun.* **2003**, *128*, 239−244.
(13) Herner, S. B.; Mahajani, M.; Konevecki, M.; Kuang, E.; Radigan, S.; Dunton, S. V. *Appl. Phys. Lett.* **2003**, *82*, 4163−4165.
(14) Ishida, K.; Miura, Y.; Hirose, K.; Harada, S.; Narusawa, T. *Appl. Phys. Lett.* **2003**, *82*, 1842−1844.
(15) Zhao, Q. T.; Kluth, P.; Winnerl, S.; Lenk, S.; Mantl, S. *Microelectron. Eng.* **2002**, *64*, 443−447.
(16) Puntes, V. F.; Krishnan, K. M.; Alivisatos, A. P. *Science* **2001**, *291*, 2115−2117.
(17) Su, M.; Li, Y.; Maynor, B.; Buldum, A.; Lu, J. P.; Liu, J. *J. Phys. Chem. B* **2000**, *104*, 6505−6508.
(18) Alberti, A.; La Via, F.; Spinella, C.; Rimini, E. *Microelectron. Eng.* **2001**, *55*, 163−169.
(19) Kang, B. S.; Oh, S. K.; Kang, H. J.; Sohn, K. S. *J. Phys.: Condens. Matter* **2003**, *15*, 67−76.
(20) Lin, S. H.; Mack, I.; Pongkrapan, N.; Fraundorf, P. *Electrochem. Solid-State Lett.* **2002**, *5*, G83−G85.
(21) Donaton, R. A.; Maex, K.; Vantomme, A.; Langouche, G.; Morciaux, Y.; Stamour, A.; Sturm, J. C. *Appl. Phys. Lett.* **1997**, *70*, 1266−1268.
(22) Lee, M. Y.; Bennett, P. A. *Phys. Rev. Lett.* **1995**, *75*, 4460−4463.
(23) Chong, R. K. K.; Yeadon, M.; Choi, W. K.; Stach, E. A.; Boothroyd, C. B. *Appl. Phys. Lett.* **2003**, *82*, 1833−1835.
(24) Murarka, S. P. *Silicide for VLSI Applications*; Academic Press: New York, 1983.
(25) *Silicide Thin Films—Fabrication, Properties, and Applications*; Tung, R., Maex, K., Pellegrini, P. W., Allen, L. H., Eds.; MRS: Boston, MA, 1996; Vol. 402.